Mechanism and Machine Theory 79 (2014) 46–63

Contents lists available at ScienceDirect

Mechanism and Machine Theory

journal homepage: www.elsevier.com/locate/mechmt

Numerical and experimental investigation of drag torque in a two-speed dual clutch transmission ☆

Xingxing Zhou [a,*], Paul Walker [a,**], Nong Zhang [a,b,1], Bo Zhu [a,c,2], Jiageng Ruan [a,3]

[a] School of Electrical, Mechanical and Mechatronic Systems, University of Technology, Sydney (UTS), Sydney, NSW 2007, Australia
[b] State Key Laboratory of Advanced Design and Manufacturing for Vehicle Design, Hunan University, Changsha 410082, China
[c] BAIC Motor Electric Vehicle Co. Ltd., Beijing 102606, China

ARTICLE INFO

Article history:
Received 7 November 2013
Received in revised form 15 April 2014
Accepted 15 April 2014
Available online 9 May 2014

Keywords:
Drag torque
Power loss
Mathematical model
Dual clutch transmission
Experimental investigation

ABSTRACT

The theoretical analysis of drag torques within a two-speed dual clutch transmission is presented in this article. The numerical models are developed to study the different sources of drag torques in dual clutch transmission. Simulations are performed in Matlab/Simulink platform to investigate the variation of drag torques under different operating conditions. Then an experimental investigation is conducted to evaluate the proposed model using an electric vehicle powertrain test rig. Outcomes of experimentation confirm that simulation results agree well with test data. Therefore the proposed model performs well in the prediction of drag torque for the transmission, and can be applied to assess the efficiency of the transmission. Results demonstrate that the entire drag torque is dominated by the viscous shear in the wet clutch pack and gear churning losses. This lays a theoretical foundation to future research on reducing drag torque and applications of drag torque in powertrain system efficiency optimization.

1. Introduction

In recent years there has been significant attention drawn towards reducing fossil fuel consumption and emissions in the automotive industry. Improvement of the overall energy efficiency of existing technologies is one of the most important subjects for developing new vehicle technologies. As a consequence of this, the development of commercially viable hybrid electric vehicles (HEVs), fuel cell vehicles (FCVs) for using in the short to mid term, and pure electric vehicles (EVs) in the long term is one of the major contributions in the automotive industry to solve related issues [1]. Pure EVs currently being used in the market are mainly equipped with single speed transmissions, with tradeoffs between dynamic (such as climbing ability, top speed, and acceleration) and economic performance (drive range). Nowadays, more and more EV researchers and designers are paying attention to application of multiple speed transmissions instead of traditional single speed transmissions, expecting to improve the EV performance. The usage of multispeed transmissions for electric vehicles is likely to improve average motor efficiency and

☆ This paper is submitted for possible publication in *Mechanism and Machine Theory*. It has not been previously published, is not currently submitted for review to any other journal, and will not be submitted elsewhere during the peer review.

* Corresponding author. Tel.: +61 2 9514 2517; fax: +61 2 9514 2655.
** Corresponding author. Tel.: +62 2 9514 2412; fax: +61 2 9514 2655.
E-mail addresses: Xingxing.Zhou@student.uts.edu.au (X. Zhou), Paul.Walker@uts.edu.au (P. Walker), Nong.Zhang@uts.edu.au (N. Zhang), zhubo@bjev.com.cn (B. Zhu), Jiageng.Ruan@student.uts.edu.au (J. Ruan).
[1] Tel.: +61 2 9514 2662; fax: +61 2 9514 2655.
[2] Tel.: +62 2 9514 2517; fax: +61 2 9514 2655.
[3] Tel.: +62 2 9514 2412; fax: +61 2 9514 2655.

http://dx.doi.org/10.1016/j.mechmachtheory.2014.04.007
0094-114X/

range capacity, or even can reduce the required motor size. The detail advantages of two-speed transmission over single speed are demonstrated in previously reported work [2].

As an important part of electric vehicle powertrain system design and optimization, it is of great importance to predict the transmission efficiency early in the design process, leading to improved powertrain efficiency as the system is refined. In addition to the design characteristics of the transmission, drag torque, acting as the sources of power losses within transmission, is affected by operating conditions, including variations in both speed and load. The total drag torque within a gear-train for any transmission is generally made up of several parts, including gear friction [3–6], windage [7–9] and oil churning [10,11]. Other important drag torque sources have to be considered as well, comprising bearings and seal [11–13], synchronizer and free-pinion losses [14,15]. If the clutch is immersed in oil, torsional resistance and its influences caused by the viscous shear between wet clutch plates should be considered as well [16,17]. Several researchers have done some specific studies regarding the drag torque within disengaged wet clutches [18–21], which will be analysed in the 2nd section.

However, in order to comprehensively improve the whole automotive powertrain system efficiency, it is necessary to consider all aspects of the transmission power losses [22]. There are only a few reported works on the entire transmission power losses [23–27], which are mostly focused on a manual transmission (MT) gear-train. There is limited, if any, published work to combine the gearbox components and wet clutch losses together to study. Especially, there is no published report on a study of an entire drag torque within wet dual clutch transmissions (DCT).

In this paper, drag torque within a two-speed dual clutch transmission is discussed. A general two-speed wet DCT is suggested to be equipped into a pure electric vehicle (EV), as shown in Fig. 1. The system under consideration is modified from a 6-speed DCT (DQ250) into a two-speed DCT. The two-speed DCT housing is made from an aluminium alloy. And the DCT is made up of two clutches, the inner clutch (C1) and the outer clutch (C2). The two clutches have a common drum attached to the same input shaft from the electric motor, and the friction plates are independently connected to the 1st or second gear. C1, shown in green, hereby connects the outer input shaft engaged with the 1st gear, and C2, shown in red, connects the inner input shaft engaged with the 2nd gear. In order to make the transmission control system simpler and save manufacture fees, there are no synchronisers in this new type of two-speed DCT. Thus, the transmission can be looked at as two clutched gear pairs, and, in this sense, shifting is realised through the simultaneous shifting between these two halves of the transmission. For this special layout, a vehicle equipped with a DCT can not only change speed smoothly with nearly no power hole, identified by Goetz [28], but also improve the EV efficiency as well.

This paper is organised as follows. In the 2nd section, the different sources of drag torque in the DCT is theoretically analysed and modelled including torsional resistance caused by viscous shear caused between wet clutch plates and concentrically aligned shafts, gear mesh friction and windage, oil churning, and bearing losses. Then experimental aspects comprising the description of the UTS test rig, and the drag torque test procedures are presented and discussed in the 3rd section. In the 4th section, simulation and experimental results are compared and analysed to validate the effectiveness of the numerical model. Finally, some significant conclusions drawn from the study are summarized in the 5th section.

2. Theoretical analysis of drag torque in wet dual clutch transmissions

The sources of power loss in a two-speed DCT, or drag torque, can be divided into five major origins: gear related meshing, windage and churning losses, bearings and oil seal related losses, concentric shaft related viscous shear losses, and disengaged

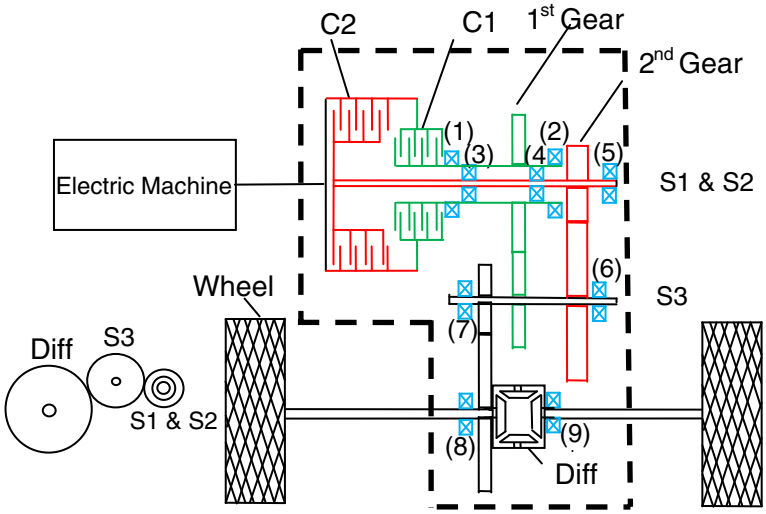

Fig. 1. Schematic of a two-speed DCT powertrain system.

wet clutch caused drag torque losses, as shown in Eq. (1). For each individual power loss source, the following formulae have been implemented in the simulation code.

$$P_L = P_{Con} + \sum P_B + \sum P_G + P_{Ch} + P_{Cl} \tag{1}$$

where P_L is total power losses in DCT, P_{Con} is power losses caused by concentric shaft drag torque, P_B is power losses caused by bearing drag torque, P_G is power losses caused by gear meshing drag torque, P_{Ch} is power losses caused by gear churning, and P_{Cl} is power losses caused by wet clutch plate drag torque.

If engaged with the 1st gear, clutch 1 is closed, while clutch 2 will be open and subsequently develop a drag torque.

$$\left(T_m - T_{con} - T_{B(1,2)}\right) * r_{1st} = T_{1st\_output\_outer} \tag{2}$$

$$\left[T_{1st\_output\_outer} - T_{GM_{1st\_pair}} - T_{B(6,7)} - \left(T_{GM_{2nd\_pair}} + T_{Cl_{C2}} + T_{B(3,4,5)}\right) * r_{2nd}\right] = \frac{T_{2nd\_output}}{r_{3rd}} \tag{3}$$

$$T_{2nd\_output} - T_{GM_{3rd\_pair}} - T_{Ch} - T_{B(8,9)} = T_{final\_output} \tag{4}$$

where T_m is motor output torque; T_{con} is drag torque caused by concentric shaft viscous shear resistance; T_B is drag torque caused by bearings; and r is gear ratio. $T_{1st\_output\_outer}$ represents the output torque of the outer concentric shaft. T_{GM} is drag torque caused by gear pair meshing, and T_{Cl} is the drag torque caused by wet clutch packs. T_{Ch} is the drag torque caused by churning. And the individual power losses can be calculated in rotational speed multiplied by drag torque:

$$P = \frac{T * n}{9550}. \tag{5}$$

For the power losses caused by concentric shaft raised shear resistance is:

$$P_{Con} = \frac{T_{con} * n_{motor}}{9550}. \tag{6}$$

The total power loss caused by bearings and gear friction is:

$$\sum P_B = \left(T_{B(1,2)} * n_{motor} + T_{B(3,4,5)} * n_{motor}\frac{r_{2nd}}{r_{1st}} + T_{B(6,7)} * \frac{n_{motor}}{r_{1st}} + T_{B(8,9)} * \frac{n_{motor}}{r_{1st} * r_{3rd}}\right)/9550 \tag{7}$$

$$\sum P_G = \left(T_{GM_{1st\_pair}} * \frac{n_{motor}}{r_{1st}} + T_{GM_{2nd\_pair}} * n_{motor}\frac{r_{2nd}}{r_{1st}} + T_{GM_{3rd\_pair}} * \frac{n_{motor}}{r_{1st} * r_{3rd}}\right)/9550. \tag{8}$$

The power loss resulting from gear windage and churning is:

$$P_{Ch} = \frac{T_{Ch} * n_{motor}}{r_{1st} * r_{3rd} * 9550}. \tag{9}$$

The overall power loss caused by clutch package is:

$$P_{Cl} = \frac{T_{Cl_{C2}} * n_{motor} * r_{2nd}}{r_{1st} * 9550}. \tag{10}$$

Similarly, if engaged with the 2nd gear, clutch 2 is closed, while clutch 1 is open.

$$\left(T_m - T_{con} - T_{B(3,4,5)}\right) * r_{1st} = T_{1st\_output\_inner} \tag{11}$$

$$\left[T_{1st\_output\_inner} - T_{GM_{2nd\_pair}} - T_{B(6,7)} - \left(T_{GM_{1st\_pair}} + T_{Cl_{C1}} + T_{B(1,2)}\right) * r_{1st}\right] = \frac{T_{2nd\_output}}{r_{3rd}} \tag{12}$$

$$T_{2nd\_output} - T_{GM_{3rd\_pair}} - T_{Ch} - T_{B(8,9)} = T_{final\_output} \tag{13}$$

$$P_{Con} = \frac{T_{con} * n_{motor}}{9550} \tag{14}$$

$$\sum P_B = \left(T_{B(1,2)} * \frac{n_{motor} * r_{1st}}{r_{2nd}} + T_{B(3,4,5)} * n_{motor} + T_{B(6,7)} * \frac{n_{motor}}{r_{2nd}} + T_{B(8,9)} * \frac{n_{motor}}{r_{2nd} * r_{3rd}}\right)/9550 \tag{15}$$

$$\sum P_G = \left(T_{GM_{1st\_pair}} * n_{motor}\frac{r_{1st}}{r_{2nd}} + T_{GM_{2nd\_pair}} * \frac{n_{motor}}{r_{2nd}} + T_{GM_{3rd\_pair}} * \frac{n_{motor}}{r_{2nd} * r_{3rd}}\right)/9550 \tag{16}$$

$$P_{Ch} = \frac{T_{Ch} * n_{motor}}{r_{2nd} * r_{3rd} * 9550} \tag{17}$$

$$P_{Cl} = \frac{T_{Cl_{C2}} * n_{motor} * r_{1st}}{r_{2nd} * 9550} \tag{18}$$

The overall efficiency of a DCT or any transmission in general can be obtained by monitoring the input and output speed and torque respectively.

$$\frac{n_{final} * T_{final\_output}}{n_{motor} * T_{motor}} * 100\% = E_{DCT} \tag{19}$$

2.1. Drag torques caused by gears

Drag torques caused by gears can be generally divided into gear meshing loss, and gear windage and churning loss. Meshing losses are a result of rolling and sliding friction in mating gears and are, as such, a load dependent loss, whilst windage and churning losses are generated from the gears rotating in fluids, and are therefore speed dependent.

2.1.1. Gear mesh

The gear meshing losses in gear pairs are dependent on both rolling and sliding friction. Methods for studying these losses reported in works [3,4,10] on theoretical analysis and modelling the friction coefficient are divided into two methods. One majority of works study the friction coefficient variation over the gear geometry and the contact force vector [5,11], which seems impractical for wide application. Other works [15] considers the loss in gear pairs only which is more compact and applicable to general simulation and practical experiments. Considering the rigorous development of British Standards [15], the model presented in the standards is chosen to calculate the gear meshing caused drag torques, as shown below:

$$p_m = \frac{f_m T_1 n_1 \cos^2\beta_w}{9549M} \tag{20}$$

where p_m is meshing power loss, kW; f_m is mesh coefficient of friction; T_1 is pinion torque, N·m; n_1 is pinion rotational speed, rpm; β_w is operating helix angle, degree; and M is mesh mechanical advantage. Meshing mechanical advantage can be calculated using Eq. (21). This equation is a function of the sliding ratios. For external gears, the sliding ratio at the start of approach action, Hs, is calculated using Eq. (22), and the sliding ratio at the end of recess action, Ht, is obtained with Eq. (23).

$$M = \frac{2\cos a_w (H_s + H_t)}{H_s^2 + H_t^2} \tag{21}$$

where α_w is transverse operating pressure angle, degree; Hs is sliding ratio at the start of approach action; and Ht is sliding ratio at the end of recess action.

$$H_s = (r+1)\left[\left(\frac{r_{o2}^2}{r_{w2}^2} - \cos^2\alpha_w\right)^{0.5} - \sin\ \alpha_w\right] \tag{22}$$

$$H_t = \left(\frac{r+1}{r}\right)\left[\left(\frac{r_{o1}^2}{r_{w1}^2} - \cos^2\alpha_w\right)^{0.5} - \sin\ \alpha_w\right] \tag{23}$$

where r is gear ratio, which can be calculated by Eq. (24); R_{o2} is gear outside radius, mm; R_{w2} is gear operating pitch radius, mm; R_{o1} is pinion outside radius, mm; and R_{w1} is pinion operating pitch radius, mm.

$$r = \frac{z_2}{z_1} \tag{24}$$

where z_2 is the number of gear teeth; and z_1 is the number of pinion teeth.

If the pitch line velocity, V, is 2 m/s ≤ V ≤ 25 m/s and the load intensity (K-factor) is 1.4 N/mm^2 < K ≤ 14 N/mm^2, then the gear meshing coefficient of friction, f_m, can be expressed by Eq. (25). Outside these limits, values for f_m must be determined by experience. K-factor can be calculated using Eq. (26). Exponents, j, g and h modify viscosity, ν, K-factor and tangential line velocity, V, respectively.

$$f_m = \frac{\nu^j K^g}{C_1 V^h} \tag{25}$$

where ν is the kinematic oil viscosity at operating sump temperature, cSt (mm^2/s); K is the K-factor, N/mm^2; C1 is a constant; and V is the tangential pitch line velocity, m/s.

$$K = \frac{1000 T_1 (z_1 + z_2)}{2 b_w (r_{w1})^2 z_2} \tag{26}$$

where b_w is face width in contact, mm. Values to be used for exponents j, g and h and constant C_1 are as follows: $j = -0.223$, $g = -0.40$, $h = 0.70$, and $C_1 = 3.239$. The coefficient varies from 0.07 to 0.03 during the simulation.

2.1.2. Gear windage and churning

As alluded before, research on gear windage had been done by Dawson [7] and Diab et al. [9] on larger high speed gears, and Eastwick and Johnson [8] conclude that the effects of gear windage loss in low and mid speed is not evident, while it becomes gradually prominent in high speed. For the churning loss, both Changenet and Velex [10] and British Standards [15] present a study for a general gear box. However, the formulas presents in Changenet and Velex [10] assumed that all the gears are submerged in the fluids, and too many parameters are required to validate to get a reasonable practical dimensionless drag torque coefficient C_m. Considering the rigours and universality of standard models, British Standards formulas are adopted here.

As shown in British Standards [15], a gear dip factor, f_g, must be considered before obtaining gear windage and friction loss. This factor is based on the amount of dip that the element has in the oil. When the gear or pinion does not dip in the oil, $f_g = 0$. When the gear dips fully into the oil, $f_g = 1$. When the element is partly submerged in the oil, linearly interpolate between 1 and 0 is used to acquire the transient gear dip factor. The primary dip factor of the final gear is 0.21. The higher the speed, the smaller the dip factor becomes. When the speed increases, it will range from 0.21 to 0.1 according to the speed. The primary depth value with 0.21 is calculated via opening the transmission, and measuring the height of shaft, gear size and the oil tube. The final 0.1 is an estimated value after debugging the model parameters and referring from a Conference paper [29]. The power loss equation for the tooth surface is named as a roughness factor, R_f. Table 12.5 of Ref. [30] presents several values based on gear tooth size. Eq. (27) is a reasonable approximation of the values from Dudley's model.

$$R_f = 7.93 - \frac{4.648}{M_t} \tag{27}$$

where R_f is roughness factor, and M_t is transverse tooth module, mm.

Gear windage and churning loss includes three kinds of loss. For those loss associated with a smooth outside diameter, such as the outside diameter of a shaft, use Eq. (28). For those loss associated with the smooth sides of a disc, such as the faces of a gear, use Eq. (29). It should be pointed out that Eq. (29) includes both sides of the gear, so do not double the value. For those loss associated with the tooth surfaces, such as the outside diameter of a gear pinion, use Eq. (30).

For smooth outside diameters,

$$P_{GW} = \frac{7.37 f_g \gamma n^3 D^{4.7} L}{A_g 10^{26}}. \tag{28}$$

For smooth sides of a discus

$$P_{GW} = \frac{1.474 f_g \gamma n^3 D^{5.7}}{A_g 10^{26}}. \tag{29}$$

For tooth surfaces

$$P_{GWi} = \frac{7.37 f_g \gamma n^3 D^{4.7} F\left(\frac{R_f}{\sqrt{\tan \beta}}\right)}{A_g 10^{26}} \tag{30}$$

where P_{GWi} is power loss for each individual gear, kW; f_g is gear dip factor; D is outside diameter of the gear, mm; A is arrangement constant, here set as 0.2; F is total face width, mm; L is length of the gear, mm; and β is generated helix angle, degrees. For helix angles less than 10°, use 10° in Eq. (30).

For a common output shaft assembly, Eq. (28) would be used for the OD of the shaft outside of the gear between the bearings, Eq. (29) for the smooth sides of the gear, and Eq. (30) for the tooth surfaces. After calculating the individual gears for each shaft assembly in a reducer, they must be added together for the total loss.

2.2. Bearing and oil seal model

As an important part of the power losses in transmission, bearing loss has been analysed by Harris [12] for a variety of bearing designs, considering both viscous friction caused torque and applied load generated torque. This work is widely accepted as the forefront on the topic, with similar results being applied in works [4,11]. And a similar bearing model is presented in Ref. [15], which is widely used in the German gear industry. Hence, the equations from the work [15] are chosen and presented below.

Load dependent bearing loss is:

$$P_{bl} = f_L F_b d_m. \tag{31}$$

Speed dependent loss is:

$$P_{bv} = \begin{cases} 1.6 * 10^{-8} f_0 d_m^3 & \nu n < 20,000 \\ 10^{-10} f_0 (\nu n)^{2/3} d_m^3, & \nu n \geq 2000 \end{cases}. \tag{32}$$

where P_{bv} is no-load torque of the bearing, only speed independent, Nm; f_0 is bearing dip factor. Factor f_0 adjusts the torque based on the amount that the bearing dips in the oil and varies from $f_{0(min)}$ to $f_{0(max)}$. Use $f_{0(min)}$ if the rolling elements do not dip into the oil and $f_{0(max)}$ if the rolling elements are completely submerged in the oil, linearly interpolate between $f_{0(min)}$ and $f_{0(max)}$. Values for the dip factor range can be found in Ref. [15].

The oil seal power losses P_{oil} are calculated from Ref. [15].

$$P_{oil} = 7.69 * 10^{-6} * V_{oil} * d_m^2 \tag{33}$$

where V_{oil} is the velocity, and d_m is the diameter. The total oil seal losses and bearing losses are expressed in P_b.

$$P_b = P_{bl} + P_{bv} + P_{oil} \tag{34}$$

2.3. Concentric shaft drag torque

The DCT has two concentric arranged shafts which connect the gears and clutches respectively. When one of the concentric shaft running, the other concentric one will run in a different speed due to the different engaged gear ratios. Therefore, there exists a relative speed between two concentric shafts, which cause viscous shear resistance. This concentric shaft shear torque phenomenon has been studied by Schlichting and presented in Ref. [31] acting as an example of Couette flow. When the DCT input speed is at 4000 rpm (test speed maximum range), Taylor's number is 779 which is smaller than the critical one 1708. Hence the assumption for Couette flow is reasonable. Therefore, the drag torque caused by concentric shafts can be expressed as:

$$T_{con} = 4\pi\mu h_{con} \frac{R_{con\_o}^2 R_{con\_i}^2}{R_{con\_o}^2 - R_{con\_i}^2} \Delta\omega \tag{35}$$

where R_o, and R_i are the inner radius of the outer shaft and outer radius of the inner shaft, respectively. $\Delta\omega$ is the relative speed between two concentric shafts. The concentric length is expressed with h. It is assumed here that the annual area is lubricated with continuous flow.

2.4. Drag torque within multi-plates wet clutches

The theories for drag torque within wet multi-plate clutches has been discussed by several authors in the past decades. In 1984, the governing equations presented by Hashimoto et al. [13] describe the flow between adjacent flat rotating plates which laid down a framework for subsequent clutch studies. Then Kato et al. [16] explained oil film shrinking between two adjacent clutch plates due to centrifugal force which is widely accepted and referred. Kitabayashi et al. [18] provide a demonstration of the drag torque which is accurate in low speed ranges, but it is poor with predicting drag torque at high speed region as it can only show the rising portion of a typical drag torque curve at the low speed region when the clearance if full of oil film. It was demonstrated by Yuan et al. [19] using the commercial computational fluid dynamics (CFD) code FLUENT. As Yuan et al. [21] then provides an improved model which has a reasonable accuracy at both low and high speeds, this drag torque model will be compared here with a new shrinking model, which is conducted by Li et al. [32] based on analytical and experimental investigation.

2.4.1. Surface tension model

Yuan et al. [19] has presented a reasonable logic to describe the phenomenon in wet clutch plates. When the wet DCT clutch packages are full of dual clutch transmission fluid (DCTF) with viscous, a schematic of a DCT clutch pack is shown in Fig. 2. Within the clutch pack, the feeding pressure (inner diameter) is approximately the same as the exiting pressure (outer diameter). The

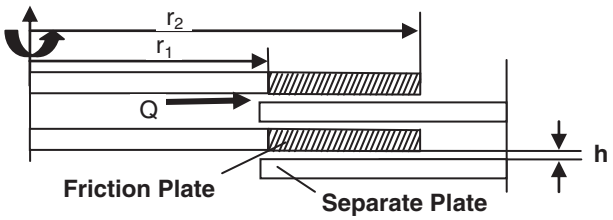

Fig. 2. Schematic of an open wet clutch.

fluid is continually pumped through the clutch pack and the flow between two clutch plates is essentially driven by the centrifugal force, while viscous shear force and surface tension forces tend to resist this motion.

The effective radius within the clutches plates is determined by the centrifugal force, viscous force and surface tension forces. When rotational speed is low, the viscous and surface tension forces are larger than that of centrifugal force and full immersion is maintained. Thus, clutch plates are full of fluid with r_2 as an effective radius. With the rotational speed increasing, the centrifugal force will increase. Once the centrifugal force is larger than the viscous and surface tension forces, the effective radius r_o will become smaller.

Via analysis of the balancing of centrifugal, viscous and surface tension forces, Yuan et al. [21] continue solving the Reynolds equation, which can be expressed in polynomial form. The effective clutch plate outer radius r_o can be achieved as the root of Eq. (35) if less than the existing outer radius.

$$\frac{\rho_{oil}\Delta\omega^2}{2}\left(f+\frac{1}{4}\right)r_o^2-\frac{\mu Q}{2\pi r_m h_c^3 G_r}r_o+\frac{\mu Q}{2\pi r_m h_c^3 G_r}r_i-\frac{2\sigma\cos\theta}{h_c}-\frac{\rho_{oil}\Delta\omega^2}{2}\left(f+\frac{1}{4}\right)r_i^2=0 \tag{36}$$

The Reynolds number is used to determine the turbulent flow efficiency f shown in Eq. (36), as shown in Ref. [21]. According to Ref. [18], the effective drag torque within the clutch packs then can be expressed as follows:

$$T_{Cl}=\frac{2\pi N\mu\Delta\omega}{h_c}\int_{r_i}^{r_o}r^3dr+\frac{0.0024\pi N\mu\Delta\omega^{1.94}}{h_c}\left(\frac{\rho h_c}{\mu}\right)^{0.94}\int_{r_i}^{r_o}r^{3.94}dr \tag{37}$$

where $\Delta\omega$ represents the relative speed between two adjacent clutch plates. From Fig. 2, $\Delta\omega$ can also mean the relative speed between the input clutch plates and the output clutch plates.

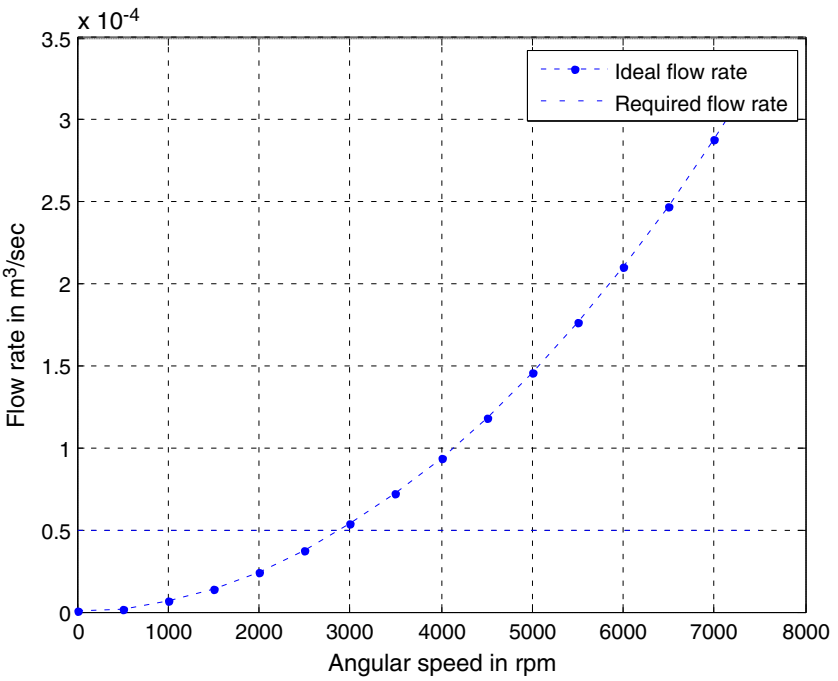

Fig. 3. Relationship of ideal and actual required flow rate.

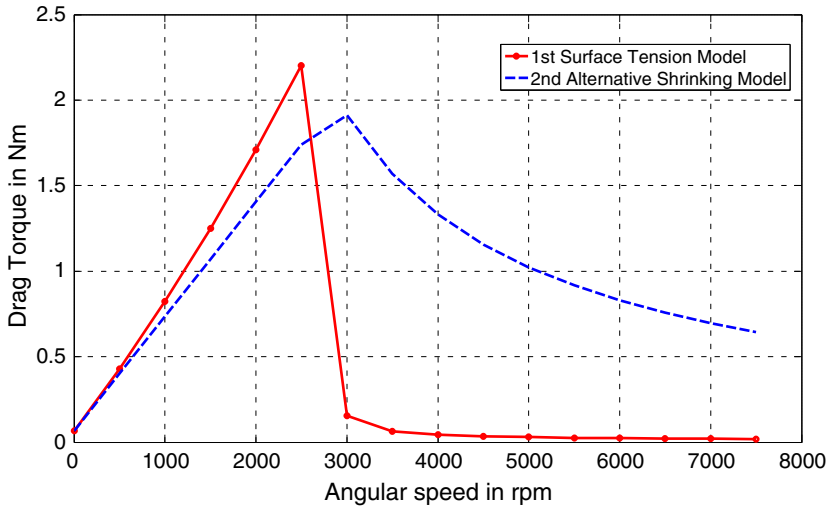

Fig. 4. Relationship of drag torque and angular velocity (2nd model) with clearance 0.20 mm.

2.4.2. Alternative shrinking model

After studying the numerically and experimentally investigated wet clutch drag torque model conducted by Yuan et al. [21], Li et al. [32] improved the model with a new way to obtain the equivalent radius considering oil film shrinking phenomenon, which will be discussed as below.

When the clearance is full of oil film, i.e., $r = R_1$, then the required input flow rate, can be obtained

$$Q = \frac{\frac{6\mu}{\pi h_c^3}\ln\frac{R_i}{R_o} + \sqrt{\left(\frac{6\mu}{\pi h_c^3}\ln\frac{R_i}{R_o}\right)2 - \frac{81\rho^2\Delta\omega^2\left(R_o^{-2}-R_i^{-2}\right)\left(R_i^2-R_o^2\right)-540\rho\left(R_o^{-2}-R_i^{-2}\right)\nabla p}{700\pi^2 h_c^2}}}{\frac{27\rho}{70\pi^2 h_c^2}\left(R_o^{-2}-R_i^{-2}\right)}. \tag{38}$$

Therefore Eq. (38) can be used to calculate the required input flow rate enable the clearance being full of oil film. It shows that the demanded input flow is influenced by the angular speed of the clutches. A trending figure to show the needed flow rate can be plotted by the simulation shown in Fig. 3.

As shown in Fig. 3, the required input flow for full oil film between clutch plates grows with the increasing of the clutch plate's speed. However, in the real practice, particular in the two-speed DCT, the actual flow rate is constant. Therefore, the oil film will shrink when the flow rate cannot meet the required flow rate with the increasing of the speed. Then we define the required flow rate as Q, the actual flow rate as Q_i, and the effective outer oil film radius as R_0.

When $Q_i \geq Q$,

$$R_0 = R_2. \tag{39}$$

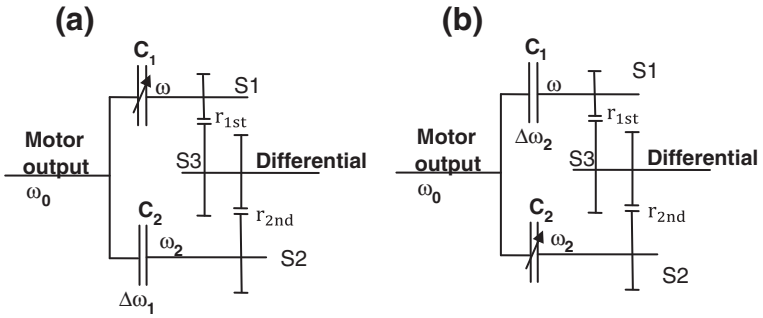

Fig. 5. Schematics of powertrain equipped with two-speed DCT, (*a*) clutch 1 closed, clutch 2 open; (*b*) clutch 2 closed, clutch 1 open.

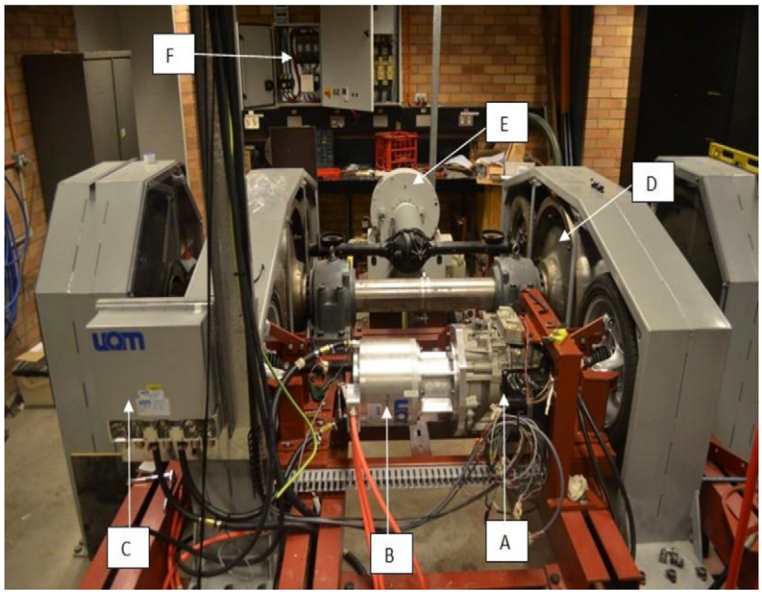

Fig. 6. Modified test rig of two-speed DCT powertrain, A) DCT; B) electric motor; C) motor controller; D) groups of flywheels; E) dynamometer; F) high voltage power supply.

When $Q_i < Q$, the relationship of oil flow rate and volume between import and export, the equivalent radius of oil can be presented as:

$$\frac{Q_i}{Q} = \frac{R_o^2 - R_1^2}{R_2^2 - R_1^2}. \tag{40}$$

Eq. (40) can be rearranged as

$$R_o = \sqrt{\frac{Q_i}{Q} R_2^2 + R_1^2 \left(1 - \frac{Q_i}{Q}\right)}. \tag{41}$$

With the obtained equivalent effective radius from Eq. (41), the drag torque can be achieved as follows:

$$\tau_{\theta z} = \mu \frac{\partial V_\theta}{\partial Z}\bigg|_{z=h_c} = \frac{\mu \Delta \omega r}{h_c} \tag{42}$$

$$T_{Cl} = 2\pi N \int_{R_i}^{R_o} r \tau_{\theta z} r dr = \frac{\pi \mu \Delta \omega N}{2h_c} \left(R_o^4 - R_i^4\right). \tag{43}$$

Comparisons are made between the two kinds of wet clutch drag torque model, and the simulation results are shown in Fig. 4. Fig. 4 shows the simulation results for the first surface tension and the second alternative shrinking model for predicting wet clutch drag torque. It shows the relationship between drag torque and angular velocity. The solid line shows the drag torque for the 1st surface tension model, and the dashed line for the 2nd new shrinking model. Both of the lines show that the drag torque is linearly increasing with the angular velocity in the first part from 0 to the peak value. However, after the speed with the peak drag torque, the drag torque reaches almost zero for the 1st surface tension model. And the drag torque for the second alternative shrinking model doesn't decrease so dramatically. In real practice, in order to continue cooling and lubricating the clutch plates, the follow rates should not be diminished, therefore, the drag torque should not be dropped down to zero in high speed, i.e.,

Table 1
DCT clutch plates' geometric parameters.

Clutch 1 plates		Clutch 2 plates		Clutch clearance	Plate number
Inner radius	Outer radius	Inner radius	Outer radius		
57.5 mm	69.5 mm	81.5 mm	96.5 mm	0.5 mm	8

Table 2
DCT gears geometrical data.

Gears	1st gear		2nd gear		Differential	
	Gear	Pinion	Gear	Pinion	Gear	Pinion
Ratio		2.0455		1.452		4.058
Pitch circle diameter (mm)	108.25	53.25	95.5	66	212.5	52.5
Tooth depth (mm)	2.875	2.875	2.75	2.75	3.75	3.75
Centre distance (mm)	80.75	80.75	80.75	80.75	132.5	132.5
Outside Diameter (mm)	114	59	101	71.5	220	60
Face width (mm)	18	16	15	15	35	37
Number of teeth	45	22	45	31	69	17
Helix angle (°)	30	30	32	32	32	32
Transverse operating pressure angle (°)	22.796	22.796	23.228	23.228	23.228	23.228
Module	2.41	2.41	2.12	2.12	3.08	3.08

higher than 3000 rpm, consequently. The second model is more likely to present actual conditions. Therefore, the second shrinking model will be chosen for further modelling and simulation within this work.

2.4.3. Drag torque within two-speed DCT

For steady state conditions, if clutch 1 (C1) is engaged, as shown in Fig. 5(a), and C2 is in open state, the vehicle is running with the 1st gear. The clutch 1 input shaft (S1) is rotating via mating of the input clutch, and its speed is the same as the output speed of EM (ω_{EM}). Then the 1st gear is engaged with the pinions in the layshaft (S3). The layshaft speed is ω_{EM}/r_{1st}. Then the layshaft (S3) will rotate with the 1st gear, causing the inner shaft (S2) to rotate as well. The inner shaft (S2) speed becomes $\omega_{EM} * r_{2nd} / r_{1st}$. Therefore, the C2 output clutch plates will rotate freely caused by the engaged 2nd gear, with speed $\omega_{EM} * r_{2nd} / r_{1st}$. The relative speed between the input clutch plates and the 2nd output clutch plates is:

$$\Delta\omega_{c2} = |\omega_{EM} * (1 - r_{2nd}/r_{1st})|. \tag{44}$$

Similarly, if the C2 is engaged, as shown in Fig. 5(b), and the vehicle runs with the 2nd gear, the relative speed between the input clutch plates and the 1st output clutch plates is $\omega_{EM*}(1 - r_{1st} / r_{2nd})$.

$$\Delta\omega_{c1} = |\omega_{EM} * (1 - r_{1st}/r_{2nd})| \tag{45}$$

Eq. (43) shows that the drag torque is directly affected by the relative rotational speed between the input and output clutch plates. Substituting Eq. (44) and Eq. (45) into Eq. (43) respectively, the wet clutch drag torque

$$T_{Cl_{r_{1st}}} = \frac{\pi\mu\Delta\omega_{c2}}{2h_c}\left(R_o^4 - R_i^4\right) = |\omega_{EM} * (1 - r_{2nd}/r_{1st})| * \frac{\pi\mu N}{2h_c}\left(R_o^4 - R_i^4\right) \tag{46}$$

$$T_{Cl_{r_{2nd}}} = \frac{\pi\mu\Delta\omega_{c1}}{2h_c}\left(R_o^4 - R_i^4\right) = |\omega_{EM} * (1 - r_{1st}/r_{2nd})| * \frac{\pi\mu N}{2h_c}\left(R_o^4 - R_i^4\right). \tag{47}$$

In transmissions, if the input speed from the motor is the same, as r_{1st} is larger than that of G2, it comes out that $\Delta\omega_{c2} > \Delta\omega_{c1}$. Thus the relative rotational speed for clutch 2 (run with 2nd gear) is always larger than that of C1 (1st gear). If the effective radius of clutch 1 and clutch 2 is the same, the drag torque engaged with the 2nd gear $T_{Cl_{G2}}$ should be larger than that of engaged with the

Table 3
DCT bearings information (mm).

Bearings	1	2	3	4	5	6	7	8
Type	Needle	Needle	Needle	Deep groove ball	Roller, angular contact	Roller, angular contact	Roller, angular contact	Roller, angular contact
Seals	No	No	No	Non-contact	No	No	No	No
Casing	External	No	No	All	All	All	All	All
ID (mm)	34.00	24.00	35.00	28.00	30.00	38.00	28.00	40.00
OD (mm)	56.00	28.00	42.00	68.00	50.00	83.00	62.00	72.00
Thickness (mm)	14.00	24.00	26.00	18.00	18.00	18.00	13.00	19.00
dm (mm)	45.90	26.05	38.61	50.78	40.83	63.29	47.14	57.52

Table 4
Dual clutch transmission fluid (DCTF) properties and test conditions.

Flow rate (m^3/s)	Oil density (kg/m^3)	Oil viscosity (N s/m^2)	Temperature (°C)
0.00005	853.4	0.0290	40

1st gear. However, the effective radius of plates in clutch 2 (C2) of this particular DCT is larger than that of C1. Therefore, the final drag torque will be determined by both the differences in effective radius and gear ratios.

3. Experimental apparatus

In this section, test facility and hardware, test instrumentation, data acquisition, and test operation will be briefly presented.

3.1. Test facility and hardware

The test facility used for this study is shown in Fig. 6 with several changes to the original UTS powertrain system test rig. The new test rig is based on an electric vehicle power train system. The original engine is replaced with a 330 V DC drive permanent magnet motor which is converted from AC high voltage electric power; the original AT transmission is replaced with a modified two-speed DCT, and the detail transmission parameters are shown from Tables 1–4. A group of flywheels and tyres are used to simulate the vehicle inertia. The dynamometer, HPA engine stand 203, a load drag on the flywheels, is used. This part of the test rig consists of two wheels contacted with flywheels, another final drive connected with shaft before the dynamometer. The DCT has a separate supply pump. The lubricate fluid will be replaced with DCTF rather than ATF. And the vehicle control unit (VCU) and transmission control unit (TCU) will be built based on dSPACE Micro-Auto Box.

During the test, the temperature is between 35 °C and 45 °C, normally approximately 40 °C. Every test point is running for about 2–3 min then taking a break. Hence it is assumed that the oil temperature does not change too much during this period.

3.2. Instrumentation and data acquisition

The test instrumentation used in this study only required measurement of the input and output speed and torque of the DCT respectively, and the DCT inside oil case temperature. Two wireless torque sensors are installed in the front half drive shafts, shown in Fig. 7, which are used to acquire the output torque data of the DCT. The wireless torque sensor is a strain gauge type sensor from ATI Technologies with a calibration error of 1%. Output shaft speed data is collected from a Honeywell digital hall effect sensor detecting the gear tooth edge on the differential. Oil temperature is collected using a k-type thermocouple sensor embedded in the transmission itself. The torque sensors are calibrated before testing, and the DCT input torque is equal to the output torque of the electric motor, which is collected by the motor feedback torque. This data was collected at a rate of 1 kHz throughout the test via a dSPACE Control Desk Recorder, and then processed in a computer.

3.3. Test operation

The test procedure used for collecting the data was the following. For a given group of operating conditions (gear, speed, motor torque, and lubricating oil temperature) the test rig was operated and stabilized last for at least 2 min. Then average one is

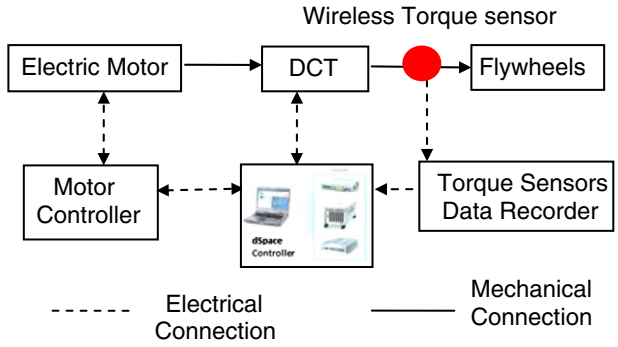

Fig. 7. Schematic test rig system.

chosen. And the error of efficiency is ±1%. Via comparing the input and output torque of transmission under different driving conditions, the difference of total drag torque power loss can be measured by a torque sensor.

4. Results and analysis

In order to validate the proposed model under the conditions of Tables 1 and 2, simulation and experimental tests are made. The following contents are the results and analysis regarding the experimental and simulation results.

Figs. 8 and 9 show the DCT efficiency for the 1st gear (a) and 2nd gear (b) from simulation prediction and during testing using constant input torque and constant input speed respectively. In Fig. 8, constant input torque (60 N·m) and various input speed from electric motor are set in this group of study. The DCT average efficiency is higher than 95% in both gears. And the efficiency in the 2nd gear shown in Fig. 8(b) is slightly higher than that of in the 1st gear shown in Fig. 8(a). Both of the efficiency decrease until they reach their bottom values respectively. After a certain speed, i.e. critical speed, the drag torque will increase gradually with the speed continually increasing in high speed. The predicted critical speeds for the 1st and 2nd gears are 2950 rpm and 2530 rpm respectively, which are very close to the speeds obtained from test results. The differences between simulation and test results are smaller, less than 0.5%. It appears that the simulation results are always a little higher than test results by 0.2% in

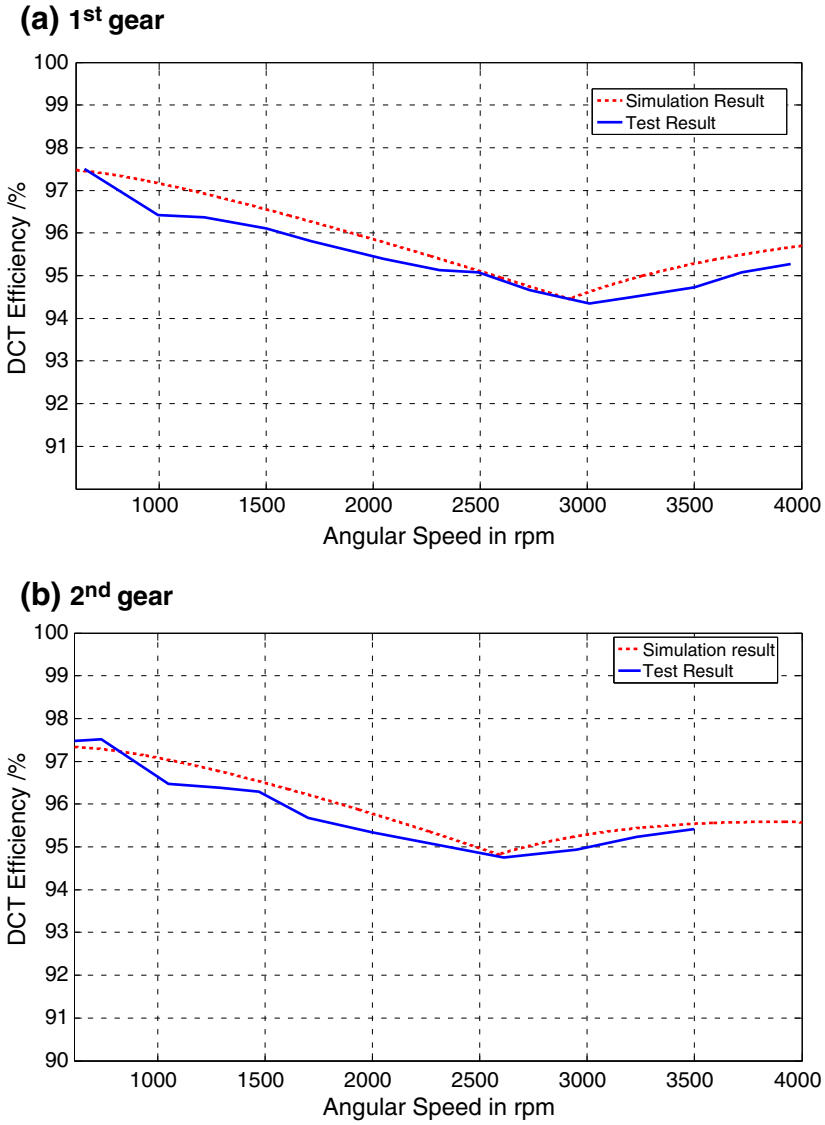

Fig. 8. Comparison of DCT efficiency between simulation and test results with input torque 60 N·m.

efficiency. It is likely that there are some other minor sources affecting the test's final results, such as the windage loss from the shaft and 1st and 2nd gear pairs by oil–air mixture resistance.

In Fig. 9, results for constant input speed (3000 rpm) and variation of input torque from the electric motor are presented. The input torque for the first gear (a) changes from 20 N·m to 60 N·m, whilst for the second ranges from 30 N·m to 60 N·m, because the second gear ratio (G2 = 5.36) is smaller than first one (G1 = 8.45), i.e., smaller gear ratio requiring larger torque to start up or maintaining stable speed. Fig. 9(a) and (b) shows that the DCT efficiency increases with the input torque continually increasing. And the efficiency in the second gear shown in Fig. 9(b) is slightly higher than that of in the first gear shown in Fig. 9(a). The differences between simulation and test results are smaller, especially in higher input torque with less than 0.5%.

From Figs. 8 and 9, it can be concluded that the results from the predicted drag torque model agree well with that from the experimental test.

Fig. 10 shows the individual drag torque losses from the simulation results at stable state. The clutch drag torque is the major loss in both gears, followed by gear churning and windage losses and bearing losses. And the clutch drag torque loss in the 1st gear is larger than that of 2nd gear if under the same input speed. The reason for that is when the 1st gear is engaged, the larger clutch (C2) will open, which generates higher torque than that of the smaller clutch (C1) when the 2nd gear is engaged.

Fig. 11 shows the percentage of losses by individual drag torque sources. It shows that the percentage of loss generated by clutch drag increases gradually before reach the critical speed. After the critical speed, the percentage of clutch drag loss drops

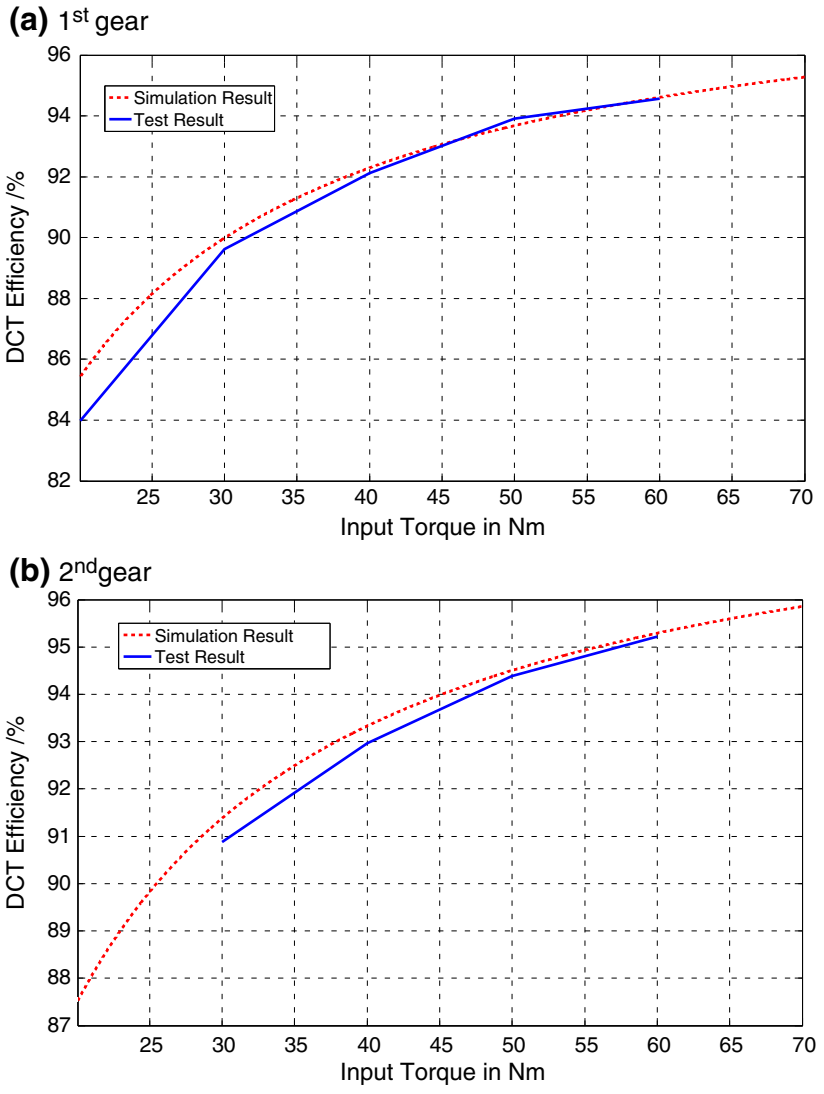

Fig. 9. Comparison of DCT efficiency between simulation and test results with input speed 3000 rpm.

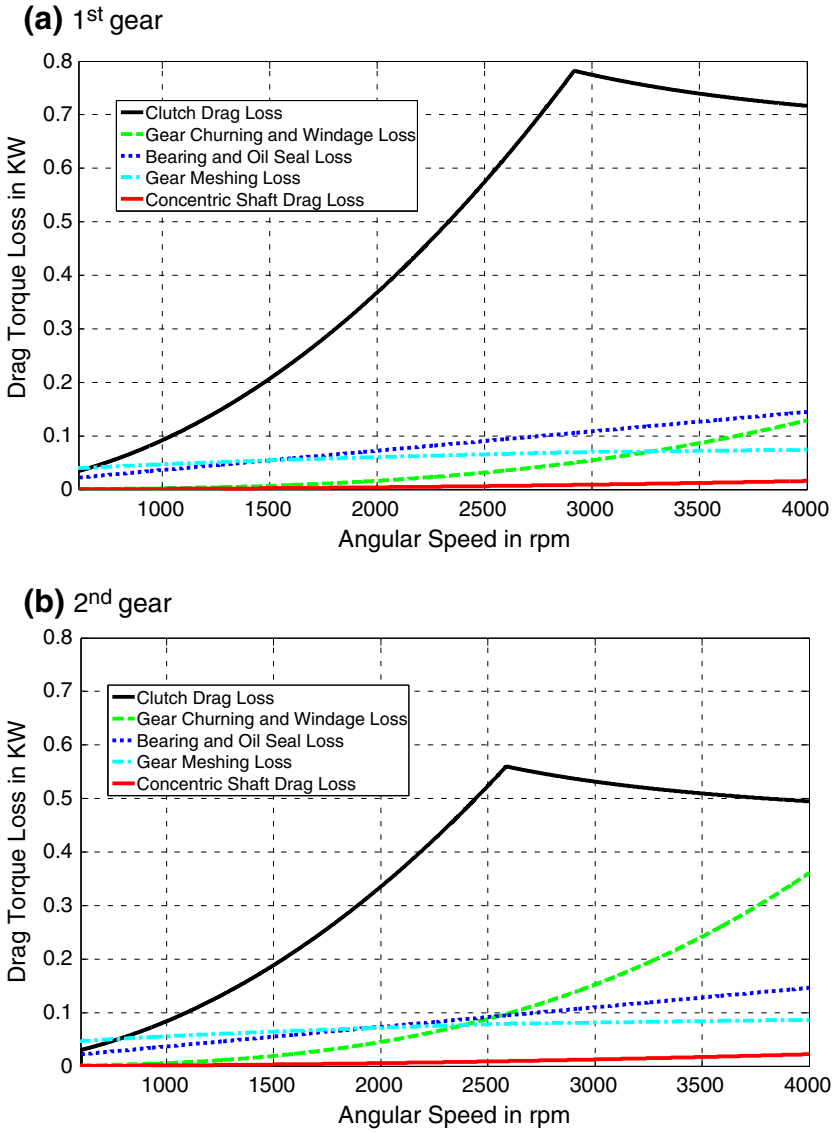

Fig. 10. Individual drag torque power loss from simulation result with input torque 60 N·m.

down slightly. It is closely corresponding with the shape in Figs. 8 and 10. The percentage of power loss in the 1st gear by clutch drag is higher than that of in the 2nd gear. And gear churning and windage loss holds the reverse condition, that is, the percentage of power losses in the 1st gear by gear churning and windage losses is lower than that of in the 2nd gear.

Fig. 12 shows the individual drag torque losses from simulation results with constant input speed 3000 rpm. Input torque from electric motor changes from 20 N·m to 70 N·m. Fig. 12(a) and (b) demonstrates that the clutch drag torque is the major loss in both gears, followed by gear churning and windage losses and bearing losses. And the gear meshing loss shares only a small part of the global resisting torque. Also the clutch drag torque loss in the 1st gear is larger than that of in the 2nd gear, which can explain why the efficiency of DCT first gear is smaller than that of second gear. Moreover, only bearing and oil seal, and gear meshing loss increase slightly with the increasing of input torque, as both represent only a small part of the total drag torque losses, which can explain why the DCT efficiency will increase with increasing of input torque at constant input speed.

5. Conclusions

The purpose of this paper is to develop a model of drag torque in a dual clutch transmission to predict its operating efficiency. After theoretical analysis of five major sources of drag torque within a two-speed DCT, this article then implemented the

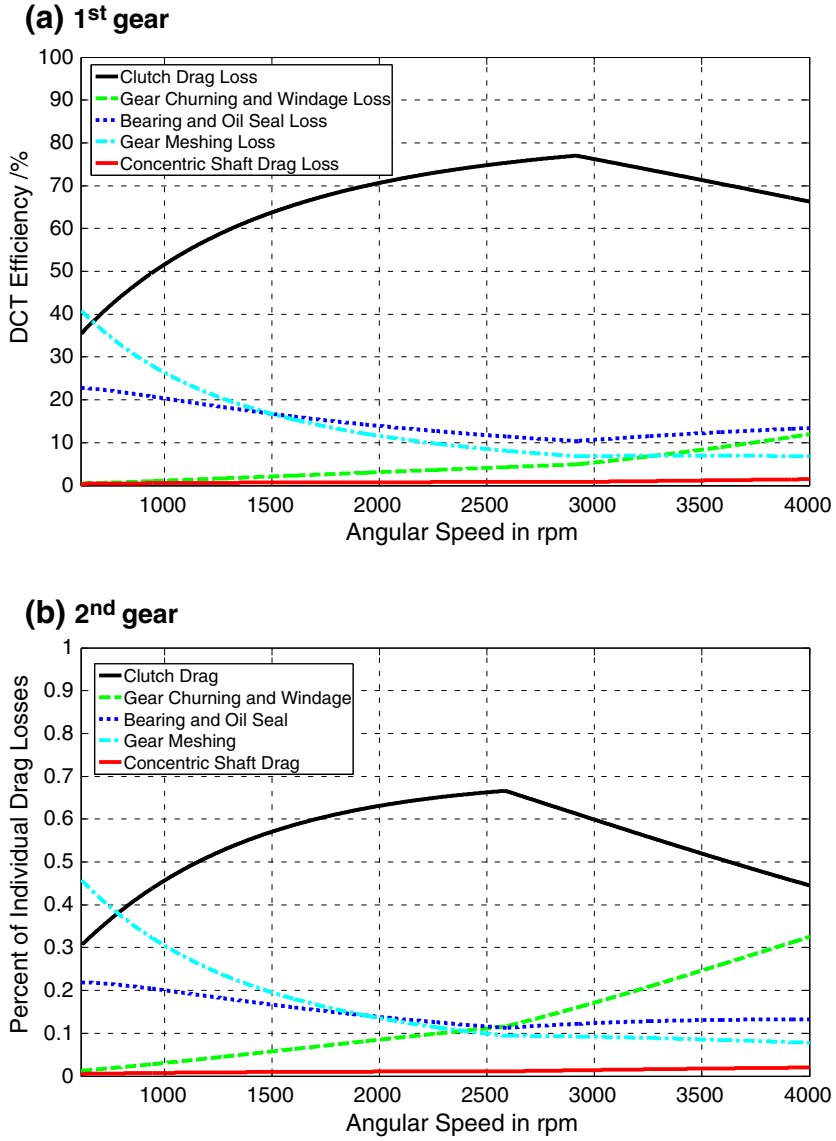

Fig. 11. Percent of individual drag torque power loss from simulation results with input torque 60 N·m.

developed mathematical model of the transmission and applied it to steady state simulation. To support the theoretical study an experimental investigation is conducted to compare the physical results with that of obtained from simulation under various operating conditions.

The test results for DCT efficiency agreereasonably and accurately with the simulation results, especially the critical speed prediction. The average error in DCT efficiency is less than 0.5%. It can be concluded that the proposed model performs well in the prediction of drag torques for the transmission, and is can be applied to assess the efficiency of the transmission. Results demonstrate that (1) the mean two-speed DCT efficiency can reach 95%. (2) And the efficiency of DCT grows with the input torque increasing, and decreases with the rise of input speed. Additionally, (3) the entire drag torque is dominated by the viscous shear in the wet clutch pack, followed by the differential gear churning and windage losses. And the gear meshing loss holds only a small contribution of the global resisting torque. (4) Moreover, when the vehicle run in the 2nd gear, the drag torque generated by clutch shear stress is smaller than that of run in the 1st gear in the same input speed. (5) The gear churning and windage losses for the 2nd gear, however, are larger than that of in the 1st gear.

This work can be looked as a reference to future research on reducing drag torque, applications of drag torque in two-speed or multi-speed electric vehicle powertrain system efficiency optimization and torque estimated shift control. With some slight adjustments according to the detail transmission layout, this numerical method for predicting the two-speed DCT drag torque can

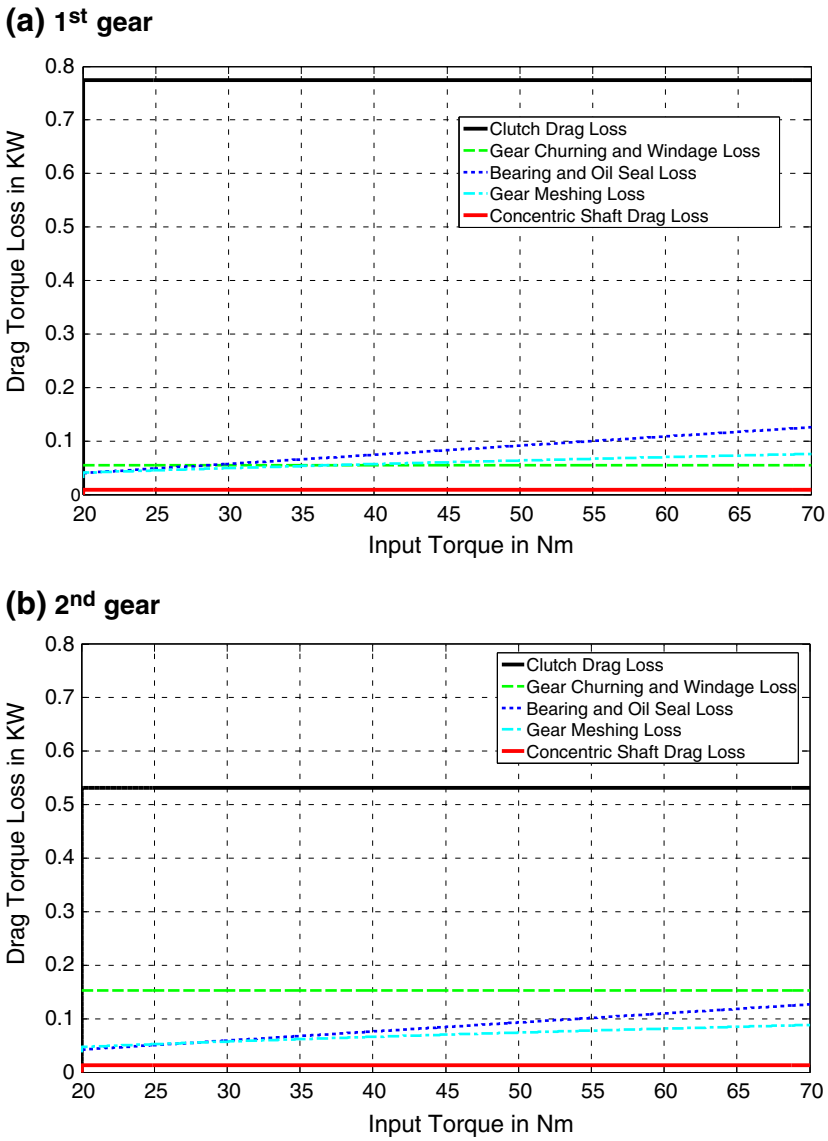

Fig. 12. Individual drag torque power loss from simulation result with input speed 3000 rpm.

also be applied to other transmissions equipped with wet clutch packages, let alone ordinary manual transmission. But the limitation of this work does not consider the influences of temperature on drag torque, which will be analysed on our future work regarding transmission thermal behaviour analysis.

Nomenclature

A_g	arrangement constant for gearing
b_w	face width in contact (mm)
C1	clutch 1
C2	clutch 2
D	outside diameter of the gear (mm)
d_m	diameter (mm)
E_{DCT}	efficiency of DCT
F	total face width (mm)
F_b	applied load (N·m)
f	turbulent flow coefficients
f_0	bearing dip factor

f_g gear dip factor
f_m mesh coefficient of friction
f_L bearing load empirical factor
Hs sliding ratio at the start of approach action
Ht sliding ratio at the end of recess action
h tangential line velocity modifying exponent
h_c clutch plate's clearance (mm)
h_{con} length of concentric shaft (mm)
j Viscosity modifying exponent
K load intensity (N/mm^2)
L length of the gear (mm)
M mesh mechanical advantage
M_t transverse tooth module
N number of frictional surface
n_1 pinion rotational speed (rpm)
n_{motor} motor speed (rpm)
P_B power losses caused by bearings drag torque (kW)
P_{Con} power losses caused by concentric shaft drag torque (kW)
P_{bl} load independent power loss (kW)
P_{bv} speed independent power loss (kW)
P_{Ch} power losses caused by gear churning (kW)
P_{Cl} power losses caused by wet clutch plates drag torque (kW)
P_G power losses caused by gear meshing drag torque (kW)
P_{GW} individual gear windage and churning loss (kW)
P_L total power losses in DCT (kW)
P_{oil} oil seal power losses (kW)
Q flow rate (m^3/s)
T_1 pinion torque (N·m)
T_B drag torque caused by bearings (N·m)
$T_{B(1,2)}$ drag torque caused by bearings (1) and (2) (N·m)
T_{Cl} drag torque caused by wet clutch packs (N·m)
T_{Ch} drag torque caused by churning (N·m)
T_{con} drag torque caused by concentric shaft viscous shear resistance (N·m)
$T_{1st\_output\_outer}$ output torque of the outer concentric shaft (N·m)
$T_{1st\_output\_inner}$ output torque of the inner concentric shaft (N·m)
T_{final_output} final output torque from DCT (N·m)
T_{GM} drag torque caused by gear pairs meshing (N·m)
$T_{GM_{1st\_pair}}$ drag torque caused by 1st gear pair meshing (N·m)
T_m motor output torque (N·m)
V pitch line velocity (m/s)
V_{oil} velocity for oil seal (rpm)
R_{con_i} outer radius of the inner shaft (mm)
R_{con_o} inner radius of the outer shaft (mm)
R_f roughness factor
R_{o2} gear outside radius (mm)
R_{w2} gear operating pitch radius (mm)
R_{o1} pinion outside radius (mm)
R_{w1} pinion operating pitch radius (mm)
r gear ratio
r_m mean radius (mm)
r_o outer radius of the clutch (mm)
r_{1st} 1st gear ratio
r_{2nd} 2nd gear ratio
z_1 number of pinion teeth
z_2 number of gear teeth
α_w transverse operating pressure angle (°)
β generated helix angle (°)
β_w operating helix angle (°)
μ viscosity of the oil ($N\ s/m^2$)
ν kinematic oil viscosity (m^2/s)
ρ_{oil} density of oil (kg/m^3)

ω_{EM} output speed of the electric motor (rpm)
$\Delta\omega$ relative speed between two concentric shafts (rpm)
$\Delta\omega_{c1}$ relative speed within clutch 1 (rpm)
$\Delta\omega_{c2}$ relative speed within clutch 2 (rpm)
∇p pressure difference between the input and output of clutch pair (Pa)

Acknowledgement

The support from Beijing Electric Vehicle Co. Ltd., NTC Powertrain, and the Ministry of Science and Technology of the People's Republic of China (2011DFB70060) is gratefully acknowledged. The first author would also like to express his gratitude to China Scholarship Council (2010613031) and the University of Technology Sydney (UTS) (436E2245) for their scholarship support.

References

[1] C.C. Chan, Electric, hybrid & fuel cell vehicles: overview, state-of-the-art, key technologies & issues, Proc. IEEE 95 (4) (2007) 704–718.
[2] X. Zhou, P. Walker, N. Zhang, B. Zhu, Performance improvement of a two speed EV through combined gear ratio and shift schedule optimization, SAE Technical Paper 2013-01-1477, 2013.
[3] Y. Diab, F. Ville, P. Velex, Investigations on power losses in high speed gears, Proc. Inst. Mech. Eng. J J. Eng. Tribol. 220 (2006) 191–198.
[4] P. Heingartner, D. Mba, Determining power losses in the helical gear mesh, Gear Technol. (2005) 32–37.
[5] S. Li, A. Vaidyanathan, J. Harianto, A. Kahraman, Influence of design parameters on mechanical power losses of helical gear pairs, J. Adv. Mech. Des. Syst. Manuf. 3 (2) (2009) 13.
[6] H. Xu, A. Kahraman, N.E. Anderson, D.G. Maddock, Prediction of mechanical efficiency of parallel-axis gear pairs, J. Mech. Des. 129 (2007) 58–68.
[7] P.H. Dawson, Windage loss in large high speed gears, Proc. Inst. Mech. Eng. J J. Eng. Tribol. 198A (1) (1984) 51–59.
[8] C.N. Eastwick, G. Johnson, Gear windage: a review, J. Mech. Des. (2008) 130.
[9] Y. Diab, F. Ville, H. Houjoh, P. Sainsot, et al., Experimental and numerical investigations on the air pumping phenomenon in high speed spur and helical gears, Proc. Inst. Mech. Eng. C J. Mech. Eng. Sci. 219 (G8) (2004) 785–790.
[10] C. Changenet, P. Velex, A model for the prediction of churning losses in geared transmissions — preliminary results, J. Mech. Des. 129 (1) (2006) 128–133.
[11] C. Changenet, X. Oviedo-Marlot, P. Velex, Power loss predictions in geared transmissions using thermal networks-application to a six speed manual gearbox, Trans. Am. Soc. Mech. Eng. 128 (2006) 618–625.
[12] T.A. Harris, Rolling Bearing Analysis, 1st ed., 1966.
[13] H. Hashimoto, S. Wada, Y. Murayama, The performance of a turbulent lubricated sliding bearing subject to centrifugal effect, Trans. Jpn. Soc. Mech. Eng. Ser. C 49 (446) (1984) 1753–1761.
[14] P.D. Walker, N. Zhang, R. Tamba, S. Fitzgerald, Simulations of drag torque affecting synchronisers in a dual clutch transmissions, Jpn. J. Ind. Appl. Math. 28 (2011) 119–140.
[15] British Standards Institute BS ISO/TR 14179-1:2001, *Gears — Thermal Capacity — Part 1: Rating Gear Drives with Thermal Equilibrium at 95 °C Sump Temperature. Part 2: Thermal Load-carrying Capacity*, 2001.
[16] Y. Kato, T. Murasugi, H. Hirano, Fuel economy improvement through tribological analysis of the wet clutches and brakes of an automatic transmission, Soc. Automot. Eng. Jpn. 16 (12) (1993) 57–60.
[17] S. Iqbal, T. Janssens, W. Desmet, F. Al-Bender, Transmitted power and energy flow behaviour of degrading wet friction clutches, Int. J. Appl. Res. Mech. Eng. 2 (1) (2012) 94–100.
[18] H. Kitabyashi, C. Li, H. Hiraki, Analysis of the various factors affecting drag torque in multiple plate wet clutches, JSAE Paper No.2003-01-1973, 2003.
[19] Y. Yuan, P. Attibele, Y. Dong, CFD simulation of the flows within disengaged wet clutches of an automatic transmission, SAE Technical Paper 2003-01-0320, 2003.
[20] C.R. Aphale, J. Cho, W.W. Schultz, S.L. Ceccio, et al., Modeling and parametric study of torque in open clutch plates, J. Tribol. 128 (2) (2005) 422–430.
[21] S. Yuan, Z. Peng, C. Jing, Experimental research and mathematical model of drag torque in single-plate wet clutch, Chin. J. Mech. Eng. 23 (2010) 1–8.
[22] G. Lechner, H. Naunheimer, Automotive Transmissions — Fundamentals, Selection, Design and Application, 1st ed. Springer, Berlin, 1999.
[23] P.D. Patel, J.M. Patel, An experimental investigation of power losses in manual transmission gear box, Int. J. Appl. Res. Mech. Eng. 2 (1) (2012) 1–5.
[24] M. Iritani, H. Aoki, K. Suzuki, Y. Morita, Prediction technique for the lubricating oil temperature in manual transaxle, SAE Technical Paper 1999-01-0747, 1999.
[25] S. Seetharaman, A. Kahraman, G. Bednarek, P. Rosander, A model to predict mechanical power losses of manual transmissions, Automob. Z. 4 (2008) 346–357.
[26] R. Per, B. Georg, S. Satya, K. Ahmet, Development of an efficiency model for manual transmissions, ATZ Worldw. 110 (4) (2008) 36–43.
[27] Y. Michlin, V. Myunster, Determination of power losses in gear transmissions with rolling and sliding friction incorporated, Mech. Mach. Theory 37 (2) (2002) 167–174.
[28] M. Goetz, Integrated Powertrain Control for Twin Clutch Transmissions, University of Leeds, 2005.
[29] L. Yang, H. Li, B. Ma, Prediction model of no-load power loss for a DSG transmission, *The 5th TM Symposium China, ICE, HEV and EV Transmission*: Suzhou, China, 2013, pp. 44–52.
[30] D.W. Dudley, D.P. Townsend, Dudley's Gear Handbook, McGraw-Hill, 1991.
[31] H. Schlichting, K. Gersten, Boundary-Layer Theory, McGraw-Hill, 2000.
[32] H. Li, Q. Jing, B. Ma, Modeling and parametric study on drag torque of wet clutch, proceedings of the FISITA 2012 World Automotive Congress, Lect. Notes Electr. Eng. 193 (2013) 21–30.